Field flow fractionation techniques to explore the “nano-world”

Catia Contado, [1,*]

Email catia.contado@unife.it

[1] Department of Chemical and Pharmaceutical Sciences, University of Ferrara, Via L. Borsari 46, 44121 Ferrara, Italy

Abstract

Field flow fractionation (FFF) techniques are used to successfully characterize several nanomaterials by sizing nano-entities and producing information about the aggregation/agglomeration state of nanoparticles. By coupling FFF techniques to specific detectors, researchers can determine particle-size distributions (PSDs), expressed as mass-based or number-based PSDs. This review considers FFF applications in the food, biomedical, and environmental sectors, mostly drawn from the past 4 y. It thus underlines the prominent role of asymmetrical flow FFF within the FFF family. By concisely comparing FFF techniques with other techniques suitable for sizing nano-objects, the advantages and the disadvantages of these instruments become clear. A consideration of select recent publications illustrates the state of the art of some lesser-known FFF techniques and innovative instrumental set-ups.

Keywords

Field flow fractionation
Nanoparticles
Quantum dots
Food additives
Drug delivery systems
Environmental nanoparticles

Introduction

Nanotechnologies and field flow fractionation (FFF) have developed almost contemporaneously. Both can be traced back to the early 1960s, when Professor J. Calvin Giddings published a short communication that clearly explained the concept of fractionation inside a thin channel in terms of Field and Flow [1], and Professor Richard Feynman delivered his famous lecture “There’s plenty of room at the bottom” [2], laying the foundations for the nanosciences.

Today, the nanosciences involve several technological fields, including chemistry, biology, medicine, physics, architecture, materials science, and engineering. In this multidisciplinary context, there is no clear agreement on the meaning of “nanomaterial.” The contexts, scopes, and applications (scientific, industrial, regulatory) specific to a given discipline lead to different definitions [3]. For an engineer, a “nanomaterial” is any material from 100 nm (1 nm = 10^{-9} m) down to the atomic level. For a pharmaceutical technologist, “nano” has replaced the term “colloid” (i.e., suspensions of particles ranging between 1 and 1000 nm in diameter), transforming the old colloidal drug delivery

systems into nanodrug delivery systems [4].

Dealing with these various definitions of “nanomaterial” is not necessarily a problem for researchers. However, the increased use of nanomaterials in many everyday products has highlighted their potential risks. Nanomaterials are neither inherently hazardous nor inherently safe for living beings and the environment. A risk assessment must determine whether a given nanomaterial is hazardous. Thus, risk assessors need a definition with clear and unambiguous criteria to identify those “nano-objects” that require further control actions.

In 2011, after carefully studying the existing international definitions [5, 6], the European Commission (EC) defined a “nanomaterial” as “a natural, incidental, or manufactured material containing particles in an unbound state or as an aggregate or as an agglomerate and where, for 50% or more of the particles in the number size distribution, one or more external dimensions is in the size range 1 nm–100 nm” [7]. What mainly distinguishes this definition from the others [e.g., International Organization for Standardization (ISO)] [8, 9] is the threshold value of 50% for the fraction of particles that should fall within the 1–100 nm size range of a *number-based* particle size distribution (PSD). Only a few other definitions contain a threshold and all these other definitions refer the threshold to a *mass-based* PSD (10% mass) [3, 5].

The implementation of the EC definition has forced the scientific community to develop or improve the existing sizing methods in order to determine *number*-based PSDs. This is not an easy task, since it involves simultaneously measuring particle size and counting the number of particles within a given size class. It is possible to convert a *mass*-based PSD, achievable with a number of techniques, into a *number*-based PSD. However, such conversions rely on assumptions that may not always apply. For example, if the particles have a very large aspect ratio, such as fibers or needles, the particle shape could be a problem [10]. There is no single clear-cut approach to reliably and accurately sizing and determining *mass* or *number*-based PSDs for a nanomaterial. The pragmatic solution is to use an ensemble of different sizing techniques, chosen according to the type of nanomaterial (NM) and its matrix [11]. The cosmetic and food sectors recommend using at least two measurement techniques, one of which should be electron microscopy (EM) [12, 13]. This is because each sizing technique determines a different dimension (geometric, hydrodynamic, aerodynamic, etc.) and different *mass*- or *number*-based PSDs.

FFF techniques number among the recommended or suggested analytical methods [10] because they can separate “nano” and “sub-micro” entities in complex and polydisperse samples.

This review seeks to highlight how some of the complex problems associated with NM characterization could be addressed by FFF implemented as separation tools and sizing techniques. Particular emphasis is given to hyphenated methods and the possible combination with ancillary or equally important analytical techniques. It is hoped that the reported examples will inspire and inform readers who may benefit from FFF’s many capabilities for analyzing nano-entities. This review concludes by considering the state of the art of FFF techniques, presenting some of the latest innovative ideas for improving the analytical methods or instrumental set-ups used to analyze and characterize NMs.

FFF techniques

FFF is a separation methodology based on flow as chromatography [14]. The column, referred to as the “channel” in FFF, is shaped like a thin ribbon with a high-dimensional aspect ratio (typical dimensions are: thickness (w): 120–350 μm, breadth: 1–2 cm, length (L): 10–90 cm). Inside the

channel flows a fluid that, because of the channel geometry and the absence of a stationary phase, is laminar, with the fastest lamina flowing in the center of the channel and the slowest lamina next to the channel walls (Fig. 1).

Fig. 1

Simplified scheme of an FFF channel operating in the normal mode, where the diffusion counteracts the action of the external field, creating sample component layers, which are transported out of the channel with different velocities, depending on the flow lamina in which they reside

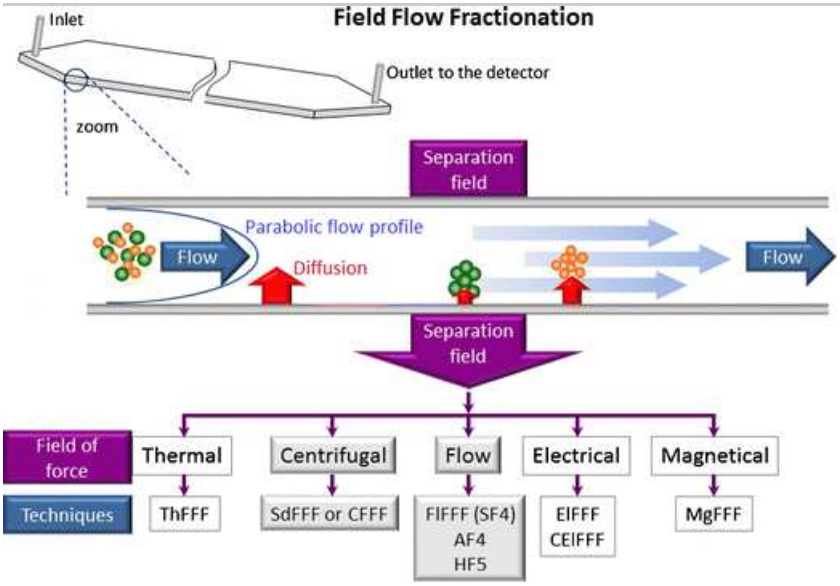

Retention and separation in the channel is caused by the action of an externally generated field of force, applied perpendicularly to the flow axis. The applied force usually drives the sample toward the bottom wall (the “accumulation wall”), while the counteracting diffusive force drives the analyte back towards the channel center. When the forces balance, a steady state equilibrium is reached and an exponential analyte concentration profile is built up. The field-induced transport and diffusion occur continuously throughout the separation. Retention ($R = t^0/t_r$) is related to the equilibrium position assumed by the analytes inside the channel ($\lambda = l/w$), whereas the separation depends on the velocity of the flow lamina in which the different analytes reside. When the sample species have diameters roughly smaller than 1 μm, retention times (t_r) increase with decreasing equilibrium layer thickness (l), and the small particles or macromolecules tend to elute first. This mode of operation is called *normal mode*.

As the particle size increases, the action of the diffusion becomes relatively insignificant in the transport process and the particles are driven by the field directly to the accumulation wall. In this case, which usually pertains to micron size particles (particles larger than 1 μm), the order of elution is determined by the extent of penetration toward the center of the parabolic flow profile (i.e., larger particles elute first). This mode of operation is called the “steric mode,” which becomes the “hyperlayer mode” when high flow velocities are used (the hydrodynamic forces generated lift particles away from the wall).

The variety of the applicable fields of force (Fig. 1) and the precise control of the field strength make the FFF techniques very versatile [14, 15]. The oldest FFF method is thermal FFF (ThFFF), where the temperature difference across the channel creates the thermal gradient necessary to induce the separation of macromolecules and particles [16]. The second oldest method is sedimentation FFF (SdFFF) [17], now called “centrifugal FFF” (CFFF) to better distinguish the sedimentation

due to the centrifugal field from that due to simple gravity (GFFF). CFFF is especially suitable for high-density particles. It can deliver high-resolution nanoparticle size separations. Flow FFF (FlFFF or F4), developed in 1976, was immediately recognized as the most versatile technique thanks to the nonspecific, hydrodynamic field applied across the channel [18]. There are now three instrumental F4 configurations: symmetric (SF4), asymmetric (AF4), and hollow fiber F4 (HF5). These configurations differ in terms of the geometrical channel shape and the way the cross-flow is applied. F4 is suitable for polymers (natural and synthetic), macromolecules, emulsion droplets, liposomes, and particles [15].

CFFF, F4, and ThFFF are commercially available (Table 1). Other techniques, developed in academia, have well-functioning prototypes but have not yet reached the market. These include electrical (ElFFF) and magnetic FFF (MgFFF) and those based on dielectrophoretic mobility and standing acoustic waves [19, 20].

Table 1

Useful theoretical expressions about the commercial available FFF techniques: relationship between the retention parameter λ and the physicochemical parameters

	Technique		
	ThFFF	**SdFFF or CFFF**	**FlFFF or F4**
External force	Temperature gradient	Centrifugal force	Cross-flow stream
Force F	$F = D\left(\frac{D_T}{D} + \gamma\right)\frac{dT}{dx}$	$F = m_{eff}\omega^2 r$	$F = f\frac{\dot{V}_c w}{V^0}$
Retention parameter λ	$\lambda = \frac{D}{D_T \frac{dT}{dx} w}$	$\lambda = \frac{D}{sGw}$	$\lambda = \frac{DV^0}{\dot{V}_c w^2}$
Achievable physicochemical parameters	$\frac{D_T}{D}$ Soret coefficient	m mass, ρ density, d_e diameter of the equivalent sphere	D Diffusion coefficient d_h hydrodynamic diameter
D: Diffusion coefficient; D_T: thermal diffusion coefficient; m_{eff} : effective mass; ω: angular rotation frequency; w: channel thickness; r: radius of curvature of the rotor; f: frictional coefficient; V_c: cross-flow velocity; V^0: : volume of the channel (void volume).			

FFF pros and cons: some comparisons

In most fields, it is mandatory to determine several physicochemical parameters characterizing a given NM, such as chemical composition, morphology, shape, surface area, crystallinity, solubility, and, of course, the average size and the PSD [21]. In this context, FFF techniques are useful as separation and/or sizing tools. Depending on the specific technique, FFF can separate sample components as a function of their mass, hydrodynamic diffusion, thermal diffusion, magnetic or electric characteristics, allowing a subsequent and more detailed characterization using complementary techniques. If the separation occurs under optimized conditions and with a sample of well-defined particles/macromolecules, FFF can also size the sample components.

In addition to FFF, other suitable tools for separating nanoparticles (NPs) include size exclusion chromatography (SEC), hydrodynamic chromatography (HDC), centrifugal liquid sedimentation (CLS), and, to a lesser extent, analytical ultracentrifugation (AUC), gel electrophoresis, and capillary electrophoresis (CE) [22]. These techniques have complementary qualities, but FFF has irrefutable advantages compared with the chromatographic techniques, especially SEC [23].

The absence of a stationary phase inside the FFF channel limits the shear forces, allowing the

separation of aggregates and fragile species. It reduces, by several orders of magnitude, the surface area available for possible interactions between the sample components and the packing material. Such interactions, which can lead to incomplete analyte recoveries, also occur inside the HDC columns, although to a slightly lesser extent because the packing material is nonporous [24, 25, 26]. Capillary HDC [27] could reduce analyte–column interactions, but is unfortunately only popular in the field of polymer separations. Compared with SEC, the absence of a stationary phase also allows more concentrated samples to be injected into the FFF channels before overloading conditions are reached.

Another important advantage offered by FFF with respect to SEC is its ability to separate particles that are largely different in size, simply by applying the opportune field gradient to the channel. SEC can obtain the same result, but only by using a sequence of columns, which unavoidably increases cost. Running costs are not a negligible factor in SEC. Replacing a column damaged by injecting an unfiltered sample, for example, costs much more than replacing an AF4 membrane (in FFF, samples can be injected without being filtered).

While the chromatographic techniques offer a large variety of column packing materials, the FFF channels (F4, ThFFF, CFFF) are compatible with many aqueous and organic solvents. This often allows samples to be kept in the native conditions and sorted in the most suitable solvent.

In terms of FFF disadvantages, it usually takes a relatively long time to set up an FFF method, and analysis usually takes between 10 to 90 min, depending on the technique and the application. As a result, SEC and HDC are often quicker. However, this is not true for CLS, where, for heterogeneous samples containing very small particles (few nm), separations can also take a couple of hours. In addition, FFF alone cannot distinguish between differently shaped particles if those particles have the same mean hydrodynamic diameter (AF4) or the same mass (CFFF). It is also unable to distinguish between primary particles, aggregates, and agglomerates.

If we limit our comparison to AF4, the most commercialized FFF technique, sample recoveries are sometimes smaller than in HDC when used for the size determination of multimodal dispersions [28]. However, AF4 shows good selectivity and size resolution. The latter is lower than that achievable by CFFF and CLS. CLS generates quite narrow PSDs but tends to proportionally underestimate the average sizes as the nominal dimension of the particles increases [29].

Thanks to the HF5 technique, FFF also recently equaled the ability of HDC and SEC to separate a dissolved form (ions/molecules) from the particulate components [30].

When FFF techniques are used as sizing instruments, the particle sizes are determined from the elution times (t_r). The size can be computed using the following equation, which governs the retention:

$$R = \frac{t^0}{t_r} \cong 6\lambda \qquad 1$$

where λ is the retention parameter reported in Table 1. The size can also be calculated using a calibration curve, obtained by injecting a series of particle standards of known dimensions and a chemical composition similar to that of the sample. FFF produces different sizes depending on the applied field. In CFFF, the particle diameter is derived from the measured particle mass, knowing the density, and assuming a spherical shape for the particle. In AF4, the size is determined using Stokes equation, making it a hydrodynamic diameter. In ThFFF, the size is determined with the diffusion coefficient D [14, 15].

As sizing tools, FFF compare with ensemble methods and counting methods. Ensemble methods examine the samples without any separation [10, 21], collecting data from a large number of particles simultaneously. These methods include dynamic light scattering (DLS) and multi-angle light scattering (MALS). Counting methods include transmission electron microscopy (TEM), scanning electron microscopy (SEM), nanoparticle tracking analysis (NTA), and single particle ICP-MS (spICP-MS).

DLS or quasi-elastic light scattering (QELS), and multi-angle light scattering (MALS) are noninvasive and easy to carry out. Unfortunately, they are based on advanced theories that cannot be easily and conclusively applied to complex polydisperse samples. DLS can measure particles in the 0.3 nm–10 μm range, but it tends to overestimate the dimensions when the particles are smaller than 40 nm [~~28~~ 29]. It is also unable to resolve particles with sizes that differ by a factor of less than 3 to 4 [31]. MALS determines the absolute molar mass and size of particles in terms of the radius of gyration, R_g (the root mean square distance of the particle's parts from its center of gravity) from the light scattered by particles in a suspension collected at different angles. The major difficulty is choosing the most appropriate model for extrapolating the size when the particle shape is unknown. The measurable sizes range from 10 to 500 nm, depending on the instrument.

Among the counting methods, electron microscopy is tedious and time-consuming because it requires so many pictures for the statistical analysis. However, it has the advantage of giving information about elemental composition or physical properties on a single particle basis.

NTA sizes the particles from the Stokes-Einstein equation. The size range is between 30 nm and 1 μm, but the lower detection limit depends on the refractive index of the NPs. NTA has better size resolution than DLS, but it tends to overestimate the number of larger particles when present in polydisperse suspensions. SpICP-MS is a new method derived from using the inductively coupled plasma mass spectrometer (ICP-MS) in the time-resolved mode. SpICP-MS does not directly determine the NP size. Rather, the particle size is calculated/estimated from the measured analyte mass by making some assumption, for example the spherical shape of the particle [32]. SpICP-MS is applied primarily to relatively simple systems containing one- or two-element particles (e.g., metals NPs) [33]. More complex multi-element NPs can be quantitatively characterized only with very fast scanning quadrupoles or time-of-flight (TOF) mass analyzers [34].

While FFF returns limited accuracy in measuring the absolute size of the NP using only the elution time without an appropriate channel calibration, this can be largely overcome if another sizing technique is placed online or offline as a detector. This hyphenation solves the limitations of each individual method because the FFF separates the original multimodal sample by size/mass. Thus, the detector, or sequence of detectors, receives almost monodisperse particle suspensions to analyze. DLS can be used to control the quality of the fractionation inside the FFF channel, quantifying the relative proportions of single particles or aggregates. The AF4-MALS hyphenation can provide important information on particle shape by evaluating the shape factor $\rho = R_g/R_h$ [35].

The coupling with ICP-OAS and ICP-MS guarantees the online determination of the concentration of specific chemical elements during fractionation, which is of fundamental importance for complex samples. However, the cutting edge of instrumental hyphenation is the coupling of FFF to spICP-MS, announced as a "proof of concept" in recent meetings [36, 37]. This coupling allows NP dimensions to be determined at very low concentration levels, by choosing one or two specific chemical elements with the common instruments, or multi-elements with fast scanning quadrupoles of TOF (time-of-flight) mass analyzers.

The choice of the detector determines the type of PDS achievable with FFF. ICP-MS, ICP-OES, and GFAAS allow *mass*-based PSDs, spICP-MS and NTA allow *number*-based PSDs, and MALS allows *light-scattering intensity*-based PSDs. The UV-vis detector, often used as an online turbidity detector, does not give a pure *mass*-based PSD because the apparent UV-absorbance is due to both light absorption and scattering [38]. It requires careful evaluation because the absorption varies with chromophore composition, and the scattering varies with light wavelength and particle size. Table 2 reports some possible FFF detectors for each dispersed nano- or micro-particle system.

Table 2

The commercially available FFF instruments, size ranges, carriers, and online detectors (connectable in sequence) for common sample types (1) [36, 37], (2) [39].The online couplings are feasible but not commercially available

Technique	Samples type	Separation size range	Eluent – carrier solution	Online detectors
FlFFF (AF4)	Biopolymers and synthetic polymers; proteins; oligomers and aggregates; conjugates; PEGylated proteins or block co-polymers; liposomes; Micelles; Virus-like particles or inactive viruses; whole serum; nanoparticles and biopolymers	Polymers: 10^4–10^9 Da Particles: 1 nm–10 μm (Depending on membrane and sample material)	All typical organic and aqueous solvents	Multi-angle light scattering (MALS) Dynamic light scattering (DLS) Refractive index (RI) UV-Vis Viscometer Fluorescence Dissolved organic carbon (DOC) Nanoparticle Tracking Analysis (NTA) *Other destructive detectors:* ICP-MS spICP-MS(1) ICP-OAS
SdFFF (CFFF)	Nano- and sub-microparticles Emulsions; gels	Particles: 10 nm–20 μm (Depending on sample material and density)	All typical organic and aqueous solvents	Dynamic light scattering (DLS) Static light scattering (SLS) Multi-angle light scattering (MALS) UV-vis absorbance *Other destructive detectors:* ICP-MS sp ICP-MS(1) ICP-OAS GFAAS(2)
ThFFF	Industrial polymers Gels Starches	Polymers: 10 kDa–100 MDa Particles: 10 nm–1000 nm	Compatible with most organic solvent systems (aqueous solvent are possible)	MALS DLS UV-vis RI Laser light scattering Fluorescence Evaporative light scattering (ELS)

Technique	Samples type	Separation size range	Eluent – carrier solution	Online detectors
				Charged Aerosol Detectors (CAD)

Applications

The versatility of the FFF techniques makes them suitable for separating all kinds of nano and micro analytes, organic and inorganic, from the initial synthesis to industrial or commercial products, from biomedical to environmental contexts. The ease of analytical determination will depend on the analyte, the matrix in which it is dispersed, its concentration (Fig. 2), and the purpose of the analysis. For example, characterizing SiO_2 NPs in an in vitro experiment that simulates digestive processes will follow a different protocol than that required to analyze SiO_2 dispersed in environmental samples. Characterizing each nano-object according to its specific nature, complexity, and source thus creates a new and important scientific challenge each time.

Fig. 2

(**a**) Key parameters affecting particle characterization; (**b**) stages of NP analysis

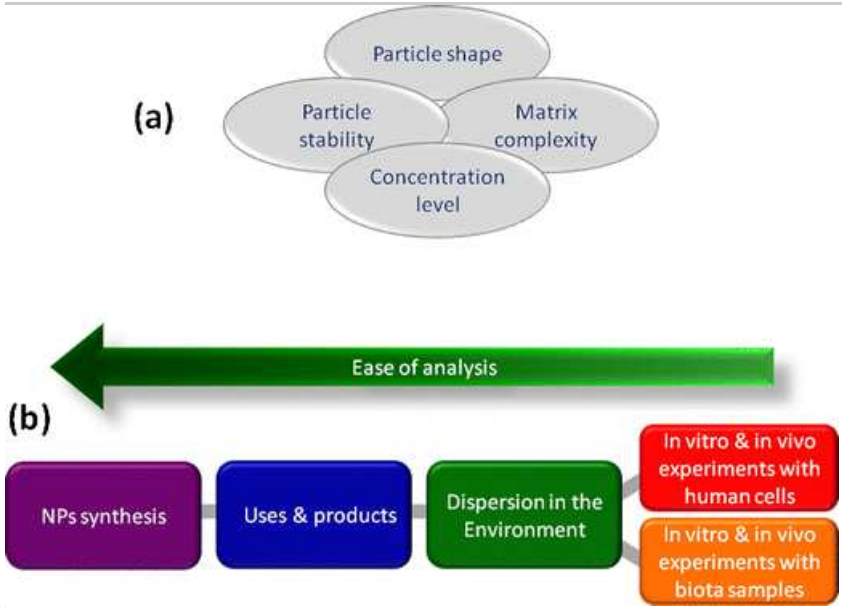

The following survey of selected applications demonstrates the concrete contributions that FFF can make to obtaining size information about NPs dispersed in complex samples. NPs are used in many research fields. However, this survey considers only those concerned with the basic physiological needs of human beings, i.e. food, health, and the environment (the preservation of the quality of water, air, and soil is a fundamental requirement for our existence). The chosen examples are mostly drawn from the last 4 y. FFF techniques are always used in combination with other analytical techniques~~.~~ (Table 3) ~~lists the analytical techniques that are used in combination with the FFF applications described herein~~.

Table 3

List of abbreviations

Techniques cited in the text or in the references

Acronym	Technique
AF4	Asymmetric flow field flow fractionation
CyElFFF	Cyclical electrical field flow fractionation
CLS	Centrifugal liquid sedimentation
DLS	Dynamic light scattering (aka PCS or QELS)
GFAAS	Graphite furnace atomic absorption spectroscopy
GEMMA	Gas-phase electrophoretic molecular mobility analysis
HPSEC	High-performance size exclusion chromatography
HF5	Hollow-fiber flow field flow fractionation
HR-ICP-MS	High-resolution inductively coupled plasma mass spectrometry
MALS or MALLS	Multi-angle light scattering or multi-angle laser light scattering
MRI	Magnetic resonance imaging
NTA	Nanoparticle tracking analysis
ICP-OES or ICP-AES	Inductively coupled plasma optical emission spectrometry or inductively coupled plasma atomic emission spectrometry
ICP-MS	Inductively coupled plasma mass spectrometry
HR LTQ Orbitrap MS	High-resolution mass spectrometer using an atmospheric photo-ionization interface
Sp-ICP-MS	Single particle inductively coupled plasma mass spectrometry
ICP-QQQ(MS)	Inductively coupled plasma triple quadrupole mass spectrometer
PCS	Photon correlation spectroscopy (aka DLS or QELS)
QELS or QUELS	Quasi-elastic light scattering (aka DLS or PCS)
SdFFF (CFFF)	Sedimentation field flow fractionation (aka centrifugal FFF)
SEM	Scanning electron microscopy
SLS	Static light scattering
SPLITT	Gravitational split-flow lateral transport thin fractionation
TEM	Transmission electron microscopy
THFFF	Thermal field flow fractionation
XRD	X-ray diffraction
UVDAD	Ultraviolet diode array
UV-vis	Ultraviolet visible spectrometer
Common abbreviations in environmental studies	
Abbreviation	Definition
ENP	Engineering nanoparticle
DOC	Dissolved organic carbon
DOM	Dissolved organic matter
MNP	Magnetic nanoparticle
HA	Humic acid
NOM	Natural organic matter

NNP	Natural nanoparticle
SRNOM	Suwannee river natural organic matter

The literature offers several informative reviews focusing on specific areas. The interested reader is referred to reviews by Runyona et al. [40] on the characterization of complex colloidal, macromolecular, and nanomaterials; Pornwilard and Siripinyanond [41] on FFF coupled to inductively coupled plasma mass spectrometry; Messaud et al. [42] on characterizations of polymers; Roda [43] on bioanalysis; and Contado [21] on consumer products and cosmetics.

Food applications

NPs are used throughout the agri-food sector from crop treatment to food storage and delivery. In some cases, the NPs are short-lived and degrade quite easily. This is true of liposomes or lipidic NPs used as carriers for active ingredients (soft NPs [44]). In other cases, workers and/or consumers may be exposed to the NPs (hard NPs), requiring a risk assessment.

Many soft and hard NPs are used during the processing of food. Both types must be carefully characterized. For soft NPs, this is because their characteristics determine the efficiency and success of the active-ingredient delivery. For hard NPs, this is because they can be long-lived and constitute an additional route of exposure if ingested in large amounts or for a prolonged time. Awareness of this new exposure route has focused the attention of the EC and EFSA on materials traditionally used as additives in food or food supplements, including SiO_2, TiO_2, silver NPs (AgNPs) [45], and carbon black. These additives should be characterized in at least three stages: as raw material, inside food matrices, and possibly under conditions simulating the digestive process [13].

Compared with the second two stages, the size characterization of “raw material” is relatively simple [13]. SiO_2 (E551) and TiO_2 (E171), for example, are usually sold as powders dispersible in water. AF4-MALS-ICP-MS supported by DLS and TEM has been used to size 11 different samples of food-grade synthetic amorphous silica (SAS) [46] dispersed in water. However, although they can obtain size distributions, these techniques have a minimum detectable size of >1 nm. Thus, because of Regulation 1169/2011 [47] on the provision of food information to consumers, they can only be used as positive tests to assess the presence of NPs inside a sample. But the presence of NPs in a sample (and their consequent detection) strongly depends on the sample preparation. Important variables, often underestimated during sample preparation, include the dispersant solution, the dispersion technique (mechanical stirring or ultrasound), and the instrumental conditions (time, temperature, energy supplied). SdFFF-UV-vis and CLS can highlight this just by comparing the separation profiles achieved under different experimental conditions [48]. Unfortunately, both SdFFF and CLS have important limitations connected to the centrifugal forces that the commercial instruments can generate. For silica particles (amorphous silica $\rho = 1.8–2.2$ g cm^{-3}), SdFFF cannot separate particles <25–30 nm. If the sample has a broad polydispersity, CLS can lower this limit to 5–10 nm, but to the detriment of the analysis time.

The ability of both SdFFF and AF4 to accurately size NPs was proven by a study performed on citrate-stabilized AgNPs suspensions in the 20 − 100 nm size range, where the results were compared with those determined by CLS and DLS [29]. However, one major limit of the FFF methods is that there are few validated procedures for simultaneously determining the average size and the concentration (PSDs) of a given sample.

There are now validated analysis protocols, based on AF4-ICP-MS, for simultaneously determining

particle size and mass-concentration distributions for SiO_2 [49] or citrate-stabilized silver NPs [50] in aqueous matrices. The protocol involves calibrating the AF4-ICP-MS with particles identical to those analyzed, injected through the channel to get a more accurate mass determination. The pre-channel calibration overcomes the common quantification problems associated with material loss during separation and with the size-dependent effects. For SiO_2, the method showed satisfactory accuracy and excellent linearity in the 0.1−25 mg L^{-1} concentration range, with limits of detection between 0.16 and 0.3 mg L^{-1} for smaller and larger particles, respectively. Externally calibrating the AF4-UV-vis-ICP-MS has also been used to analyze TiO_2 in food or personal care products, where the calibrants were rutile TiO_2-NPs standards [51]. The online calibration method was promising for quantitative determination of TiO_2NPs in moisturizing cream.

The idea behind setting up validated procedures on pristine NPs in simple matrices is that they could eventually be transferred to more complex samples. But this goal is made more challenging by the huge variety and composition of food matrices in which NPs could be embedded, and by the wide range of possible NP concentrations. AF4-ICP-MS can sort the NPs and determine silver concentrations in the 0.7–29.5 × 10^3 μg L^{-1} range (dynamic linear range 10–1000 μg L^{-1} and LODs < 28 ng L^{-1}) in a number of aqueous beverage and complex nutraceutical samples [52]. Sample preparation is one of the major challenges of NP analysis in a food matrix. Sample preparation needs to extract the NPs from a given matrix without introducing artifacts that modify the original PSD. SdFFF-UV-vis has been used to compare the fractograms, and the derived PSDs, produced by the pure SiO_2 powders and the SiO_2 particles extracted from a nearly silica-free instant barley coffee powder, previously enriched with the known SiO_2 particles [53]. The verified extraction protocol was applied to commercial products (cappuccino powder mix and a food integrator) containing SiO_2, using SdFFF-GFAAS offline coupling to monitor the results of the size fractionation [53]. Elsewhere, AF4-ICP-MS has been used to quantitatively evaluate important parameters affecting the sample preparation, such as the matrix-to-solvent ratio, the use of organic solvent for defatting, the sonication time, and food cooking procedures, mimicking real-life actions [54]. By converting the *mass*-based PSDs obtained via AF4-ICP-MS, researchers finally achieved *number*-based PSDs, as required by the regulators [7], for TiO_2 particles found in 24 food products and three personal care products. The results were comparable with those achieved via spICP-MS and SEM, although image analysis software limits meant that the smallest particles (<20 nm) were excluded, introducing a significant bias into the SEM distribution [46, 55].

AF4-ICP-MS in combination with DLS, EM, GEMMA was useful for evaluating the stability of a tomato soup spiked with SiO_2 to create a reference material for silica analysis. Indeed, another key challenge in the drive to create validated procedures is the lack of appropriate reference materials for the analysis of real food samples. This is true even considering the existing SiO_2 standards, for which the exact concentrations must be determined before their use [49]. The soup matrix was homogeneous and stable enough to allow long-term storage and distribution at room temperature [56]. This is a good result, considering that silica acts as a clarifying agent, leading to considerable precipitation of food components.

An AF4-ICP-MS method was in-house validated for the determination of AgNPs in a lean chicken meat paste, which was deliberately spiked with PVP-stabilized AgNPs to create a food reference material. The AgNPs were isolated from the meat by enzymatic digestion and separated by AF4 with recoveries of around 80% [57]. By comparing the bulk analyses with the results of the AF4 separation and spICP-MS, it was possible to identify the non-nano Ag fraction, most likely ionic silver, bound to organic constituents of the enzymatic meat digestate [58]. The method fulfills the requirements for determination of NPs in a food matrix [59], showing repeatable and intermediately reproducible determination of AgNP mass fraction and size. However, the determination of AgNPs

deserves attention since they tend to chemically transform (to dissolve) and to agglomerate/aggregate [58].

Food simulants are often used to assess the release of NPs from nano-enabled food-contact materials. In theory, this should guarantee a more accurate and reproducible detection, characterization, and quantification of NPs, allowing researchers to distinguish them from ionic species. Unfortunately, the conclusions of such studies are often contradictory because NPs are extremely diluted and unstable in certain food simulants. AF4-MALS supported by other analytical techniques (ultrafiltration, EM, and spICP-MS) was useful for investigating the stability of AgNPs spiked in water, 10% ethanol, and 3% acetic acid. Very minor to no changes in the physicochemical properties of AgNP were seen in water and 10% ethanol, while 3% acetic acid induced significant oxidative dissolution of AgNP to silver ions [60]. The AF4-MALLS method was also used to monitor the possible release of carbon black NPs, incorporated at two concentration levels in low-density polyethylene (LDPE) and polystyrene (PS) plastic packaging material, in contact with simulants, simulating long-term storage with aqueous and fatty foodstuffs. The method ascertained that carbon black NPs did not migrate in the simulants (LOD of 12 $\mu g\ kg^{-1}$) and it successfully differentiated the NPs from extracted polymer chains [61].

Biomedical applications

In the pharmaceutical and medical fields, the NPs encountered can be broadly divided into therapeutic and diagnostic nanosystems. A recent paper nicely illustrates AF4's role in analyzing a list of pharmaceutically relevant samples, including synthetic systems (NPs), polymeric self-assemblies and macromolecules, liposomes, proteins, and viruses [62]. Zattoni et al. have reported other specific applications of AF4 coupled to light scattering detection systems, where different NP types (lipidic particles, organic polymer particles, biopolymer particles) are analyzed to determine size, stability, and drug-release capabilities [63]. AF4 is not the only useful technique in these sectors. SdFFF can also be used to separate and study drug delivery systems [64, 65, 66].

In the field of drug delivery and drug carrier systems, quantum dots (QDs) play a prominent role because of their high efficiency [67]. They are very small particles (0.5–3 nm), which means that their size characterization can be quite difficult during synthesis [68, 69, 70, 71] and storage [72]. For biological applications, their surface is usually functionalized with appropriate recognition units. This reaction increases their hydrodynamic sizes but makes them superficially delicate and sensitive; nevertheless AF4, due to its intrinsic softness, can successfully separate them [73, 74]. The UV-vis detector is not so strongly recommended for this kind of application. Despite excellent detection capabilities due to the high absorption of the UV radiation, the signal is unspecific, especially when the sample contains a mixture of different QDs or NPs [73, 74]. Thus, it is recommended that AF4-UV-vis be used in biological applications only for well-defined chemical environments. The fluorescence detector could be a better option for increasing the signal's specificity [75], but the online coupling of AF4 with the ICP-MS is surely the most powerful combination in terms of sensitivity and specificity. This method has been successful, for example, in in vitro studies of the uptake of AgNPs by cells [76]. A similarly powerful combination involves the more expensive ICP-QQQ(MS). AF4-ICP-QQQ(MS) performed well when applied to the synthesis of CdSe/ZnS QDs coated with an amphiphilic polymer [75] and bioconjugated with monoclonal IgG antibody [77], coexisting in heterogeneous suspensions. Under optimized experimental conditions, AF4 fractionated the unreacted QDs and bioconjugates, allowing accurate online elemental molar determination, including sulfur S, for each peak detected by AF4 in each synthesis route. It thus identified unreacted QDs, bioconjugates [77], and all separated species, including unexpected ones [75].

Although AF4-ICP-MS is undoubtedly advantageous, the simple instrumental configuration of AF4-MALS is sufficient in some studies. The AF4-MALS coupling can be very useful for (1) studying surface interactions (e.g., between TiO_2, ZnO, CuO, and NiO NPs and lactate dehydrogenase and cytokines [78]); (2) monitoring the increase of the hydrodynamic particle diameter and the aggregation caused by variations in pH, temperature, and ionic strength, as in the case of AgNPs and cytochrome *c* (CytoC) [79] or AuNPs and polyethylene glycol (PEG) [80]; and (3) performing a structural analysis of secondary NPs with adsorbed proteins, a very significant factor for in vitro toxicity assessments, since different NPs' geometric structures exhibit different cytotoxicity and bioactivity in vitro.

The analytical problem determines the optimal instrument configuration. Expensive detectors are not always necessary. Sometimes, as mentioned above, fluorescence [75], refractive index (RI) [69, 71, 81, 82], UV-vis [70, 71, 83, 84], or scattering [85, 86] detectors can be as equally useful. The following examples have all been used to analyze iron oxide NPs. These magnetic NPs are used as biosensors, as contrast-enhancing agents in MRI, and as site-specific drug delivery agents in tumor therapy [87]. AF4 was combined with an RI detector [81] to monitor the stability, over a 3-mo timeframe, of γ-Fe_2O_3 core NPs coated with a layer of silica and functionalized with poly-2-(dimethylamino)ethyl methacrylate (PDMAEMA). AF4-RI could distinguish magnetic iron oxide NPs loaded in cationic block copolymer micelles from small particles, unbound micelles, and DNA fragments, which arose when the vectors disintegrated during synthesis of the hybrid polymer-magnetic micelles (magnetopolyplexes) [82]. AF4-UV-vis determined the PSDs and, when combined with magnetic fractionation, contributed to the magnetic characterization of the iron oxide NPs [83]. SF4-UV-vis was useful in determining the strength of the SPIO NP–protein interaction [84], a physicochemical parameter unconnected to particle size. The strength of the NP–protein interaction was evaluated by comparing the SPIO NPs collected after centrifugation with those separated by SF4. The SPIO NP–protein complexes injected into SF4 dissociated continuously under the nonequilibrium separation condition, so that only those proteins with sufficiently slow dissociation rates were collected with the NPs in the eluent of SF4, whereas proteins with good affinity for the SPIO NPs were collected after centrifugation, regardless of the dissociation rates of the complexes [84]. Elsewhere, researchers have used AF4-MALLS to size different hydrophobic oleic acid-stabilized monodisperse SPIO nanocrystals, synthesized in aqueous media for potential in vivo MRI contrast applications [85]. AF4-MALLS allowed also the selection of the formulation containing the smallest particles with the narrowest polydispersity index and with remarkable storage stability over time. AF4-DLS has been used to demonstrate that starch-modified Fe_3O_4 NPs dispersions can be achieved with a prevalence of particles <100 nm, and that they can be stable up to 70 °C, allowing their use in the treatment of degenerative cartilage diseases [86].

Thanks to their density (5.18 g cm^{-3}), Fe_3O_4 magnetic NPs can also be characterized using SdFFF-UV-vis. Dou et al. [88] have used SdFFF-UV-vis to study the influence of synthesis parameters on size distribution of Fe_3O_4 MNPs and Fe_3O_4-deposited multi-walled carbon nanotubes (Fe_3O_4@MWCNTs) synthesized using an ultrasonic co-precipitation method.

Polymeric nanosystems, the size range of which is wider than in other sectors [64, 65, 66], play an integral role in advancing drug-delivery technology by allowing the controlled release of therapeutic agents in constant doses over long periods, as well as cyclic dosage and the tunable release of both hydrophilic and hydrophobic drugs.

In this field and as an alternative to the SEC technique, AF4 (often coupled to MALS and DLS) has been used to determine the molar mass distribution of the polymers. One example is the

characterization by AF4-MALS and RI of poly n-vinyl formamide (polyNVF) [89]. Another example is the characterization by AF4-MALS-DLS of novel biodegradable polyurethanes [90]. Here, pH-responsive polymers containing different ionic segments in the backbone were used to create NPs that were sensitive to pH changes in different parts of the human body. AF4-DLS has also been used to monitor the increase of particle diameter during PEGylation of human serum albumin (HAS) NPs and to determine the particles' PEGylation degree, by separating the NPs from dissolved polyethylene glycol (PEG) [91]. Engel et al. have reported one of the few AF4-MALS validated methods in the drug delivery field [92]. NPs composed of poly(DL-lactide-co-glycolide) (PLGA) were formulated as colloidal drug carriers to improve the bioavailability of poorly soluble drugs through oral administration. The AF4-MALS method was validated for determining NP content in solid dosage forms and for quantifying particle release during dissolution testing. DLS and SEM detected the presence of unaltered PLGA-NPs after dissolution testing.

AF4-MALS and AF4-DLS allow the measurement of geometric (R_g) and hydrodynamic (R_h) radii [i.e., the shape factors (R_g/R_h)]. They can thus greatly contribute to characterizing nonspherical micro- and nanoparticles, which are important because they interact with biological systems in surprisingly different ways from their spherical counterparts [93]. Notably, AF4 also lends itself to the separation of gold nanorods of different shapes, as shown in [94], where gold nanorods were separated into subpopulations with aspect ratios, sizes, and shapes that were more narrowly dispersed than in the original population.

As an interesting appendix to this biomedical section, we can consider a recent application of the AF4-ICP-MS method in the field of artificial implants. The new hips constructed to replace surgically damaged hip joints are made from plastic, ceramic, and metal materials. But metal-on-metal (MoM) arthroplasty has led to poor outcomes for some patients since it can generate micro- or nano-size metal wear particles containing Cr, Co, or other elements. The current analytical methods do not provide sufficient information about the size or composition of the wear particles generated in vivo. In contrast, AF4-ICP-MS analysis of enzymatically digested hip aspirate samples has allowed researchers to investigate metal protein binding and to determine the size (40–150 nm) and composition of wear metal particles present in serum and hip aspirates from MoM hip-replacement patients [95].

Environmental applications

The atmosphere, hydrosphere, lithosphere, and even biosphere have always contained NPs as a result of chemical, photochemical, mechanical, thermal, and biological processes. These natural NPs (NNPs) also include those formed spontaneously as a result of the human activities (mining, industrial processes, and production of wastewaters and waste). Naturally occurring colloids are defined as solid particles with diameters between 1 and 1000 nm. Studies of these particles focus on their fate and transformation, their role in the atmosphere's chemistry, and in the transport of micropollutants. The most studied systems are inorganic minerals (e.g., iron oxides), organic biopolymers [e.g., dissolved organic matter (DOM)], microorganisms, and, due to the increased use of nanotechnological products in the last decade, engineered NPs (ENPs) released into aquatic and terrestrial environments. In this field, FFF techniques have been used to estimate sizes and PSDs, in part thanks to specific detectors, the choice of which is dictated by the research aims. This was described in detail in a recent paper on natural colloids and natural and manufactured NPs characterized via AF4 [96].

In this sector, FFF techniques are increasingly combined with element-specific detectors, such as ICP-MS, HR-ICP-MS, spICP-MS, and ICP-OES. This combines FFF's particle-size separation

capabilities with element specificity. However, the use of UV-vis, fluorescence, and/or scattering detectors (MALS and DLS) is common in a number of practical cases. AF4-ICP-MS has been widely used to study the effects of important experimental variables (pH, ionic strength, redox conditions) that must be controlled when preparing natural colloids for analysis. When the natural colloids are extracted from the environmental matrix, it is extremely important to consider the ionic composition and pH [97, 98] of the extracting solutions. This is required to maintain colloids in their native state, preserving their natural PSDs and their elemental chemical composition, and to avoid altering the interactions of the NPs with trace metals. This is particularly true when the environmental matrix contains natural organic matter (NOM), which could modify its association with iron (Fe) [99]. AF4-UV-vis and a fluorescence detector can be used to easily study the redox conditions, the variation of which can change the oxidation state of some elements (e.g., ferrous iron can form colloidal iron oxide) [100].

Researchers often use AF4-UVDAD-fluorescence-ICP-MS or simply the AF4-ICP-MS coupled systems to understand the role of colloids or NPs in the transport of metal ions and nutrients (e.g., phosphorus P). They do this by matching the AF4 separation profiles of the macromolecules (NOM), NPs, or colloids with the profiles of the trace metals [101, 102, 103, 104]. The main challenge here is quantifying the phosphorus, since colloidal P in natural waters typically occurs at low concentrations ($\mu g\ L^{-1}$ range). This problem can be overcome by using the more powerful AF4-HR-ICP-MS system [105].

The distinction between dissolved metals and stable metal–ligand complexes is equally important for the transport of metal ions by NPs and colloids. AF4 and HPSEC can both be used to separate these entities according to size. However, the presence of inorganic colloids falsifies the HPSEC results because HPSEC cannot differentiate between NOM and iron-organo mineral colloids [104]. AF4-ICP-MS allows an online chemical composition to be achieved even when several elements are selected (Fe, Al, Ti, Pb, Cu, Ni, As, U, and rare earth elements).

When the composition of the sample is well-defined, as with Fe_2O_3 NPs uncoated and coated with HA or Suwannee River natural organic matter (SRNOM), AF4-UVDAD and AF4-QELS are sufficient to assess particle stability. This was demonstrated by Chekli et al. [106, 107], who considered different groundwater conditions (i.e., pH 6–8 and high ionic strength) to evaluate the use of Fe_2O_3 NPs as soil/water remediation tools.

The contamination of the environment by ENPs poses a new challenge. But it is very difficult to discriminate between NNPs and ENPs. They can have very different concentration levels, requiring additional concentration strategies [108], or they can contain the same elements. AF4 equipped with a series of online detectors (UV-vis-MALLS-ICP-MS) was used in studies to mimic a possible soil contamination by metal NPs (AuNPs). Multiple detection is recommended because the available MALLS software does not account for the unusual scattering behavior of the metal ENPs due to the plasmon resonance effect [109].

AF4-ICP-MS can distinguish between the isotopes of a given element. Gigault and Hackley [110] have therefore proposed determining the natural isotopic signature of an estuarine sediment reference material. Then, after placing the sediment in contact with a suspension of isotopically enriched ^{109}AgNPs, the level of ^{109}Ag enrichment can be detected. This methodology is still at the "proof of principle" stage, but it could be very useful in distinguishing ENPs from NNPs made of the same chemical element but with different isotopic compositions.

AQ1

Many methods for directly detecting and quantifying ENPs in the environment have not been

validated. The only exception is the complete validation model, which uses AF4-ICP-MS to quantify the releasable AgNPs and AuNPs in aqueous matrices (tap water and domestic waste water) [111]. One study has highlighted the tendency of Ag ENPs to agglomerate in artificial seawater, which can be tackled in detail by using AF4-UV-vis combined with the spICP-MS [112]. This study was carried out as a function of temperature, dissolved organic matter, and salinity under realistic testing conditions of light cycle and agitation. It demonstrated that the kinetics of the agglomeration process are affected by the presence of organic material (alginate or HA). For TiO_2 NPs, researchers have also observed that adsorption of NOM onto the particle surface can modify particle stability and aggregate structure [113]. For AgNPs coated with polyvinylpyrrolidone (PVP), a type of organic material commonly used as a stabilizer in commercial products, researchers have also observed variations in ENP reactivity and an overestimation of their primary size (demonstrated by AF4-UV-vis and offline HR-ICP-MS) [114].

To conclude this environmental section, we can consider some AF4-ICP-MS applications for evaluating the potentially toxic effects of ENPs, either in their NP form or as they slowly dissolve, releasing ions. AF4-ICP-MS has been used to monitor differences in the AgNPs' dimensional profiles, which are caused by the action of the organic matter (DOC) or UV light. An observed decrease of AgNP toxicity for *Daphnia magna* was attributed to the dissolution or aggregation of the AgNPs, especially for high values of the media conductivity [115, 116, 117]. In turn, the possible settling of the AgNP clusters could impact the sediment and aquatic organisms. FFF-ICP-MS and spICP-MS have detected measurable silver concentrations in *Lumbriculus variegatus*. In this study, AF4-ICP-MS detected the presence of Ag in tissues (LOD of approximately 10 μg/L). spICP-MS was then used to confirm this presence at a higher level of sensitivity [118]. AgNPs could have an impact on aquatic organisms at low concentrations too. AF4-ICP-MS and NTA have detected the presence of a significant portion of dissolved silver and a mixture of single and AgNPs agglomerates in water, to which the tadpoles of bullfrogs (*Rana catesbeiana*) were exposed, and in the tadpoles themselves. This supports the idea that bioaccumulation can disrupt five TH-responsive targets [119].

Implementation of methods and instruments

To meet new research requirements and changing practical needs, there is continuous development and improvement of FFF methods and the related commercial instruments, in terms of material implementation, operation modes, interface with other instruments, and, of course, software updates. NP analysis has also driven progress in this area. This section considers some of these advances.

AF4

Calibration for sizing

AF4 is undoubtedly the most popular FFF technique for simultaneous separation and size determination of polydisperse macromolecules, colloids, and NPs. AF4 is often coupled online to additional detectors, which give orthogonal information on particles sizes. But hydrodynamic sizes can also be computed by accurately measuring the retention time t_r from a fractogram (Eq. 2). The channel thickness w is an important experimental parameter in this simplified equation, and it must be carefully determined to allow accurate size determination.

$$d_h \cong \frac{2V^0 kT}{w^2 \pi \eta t^0 \dot{V}_c} t_r \qquad 2$$

The channel thickness is usually measured by injecting a standard with a known diffusion

coefficient (D) or hydrodynamic diameter (d_h). However, its accurate determination is a challenge due to uncertainties arising from the membrane's compressibility, which may vary with experimental conditions. Dou et al. [120] have systematically investigated how the standard's size and type influence the measurement of w, showing that steric effects and the particle–membrane interactions by van der Waals or electrostatic forces may cause measurement errors. Ideally, w should be measured under the same conditions as the sample analysis, and measured each time there is a change in the experimental conditions including the composition of the carrier liquid [120]. A preferred method is to calibrate w by spherical standards of tabulated diffusion coefficients/known size, using the same flow rates and carrier composition as the sample, without changing the carrier after sample analysis.

Constructing a calibration curve (D or d_h versus V_r) is one practical solution to avoid having to determine w. The calibrants should be a series of standard NPs covering the whole range of sizes and separated [97]. Although using a calibration curve mitigates w's contribution, calibration can also lead to erroneous results. When the unknown sample contain particles of different chemical compositions [121] or different surface chemistries to the NPs used for calibration [122, 123], different attractive van der Waals forces can occur between the NPs and the accumulation wall (membrane surface) [124], causing a distorted retention.

For complex and heterogeneous samples, it can be extremely beneficial to use an additional online sizing detector, but the user must be aware of their limitations in order to avoid erroneous results. DLS, for example, becomes increasingly ineffective when the particle size approaches or exceeds ≈ 100 nm. This is because it is difficult to accurately measure autocorrelation decays for more slowly diffusing particles in a flow-cell configuration. As another example, MALS does not account for the strong optical absorbance associated with some metal NPs [124].

Although noted above as a disadvantage, the high sensitivity of AF4 to van der Waals forces can be transformed into an advantage if it is used to measure these forces. The determination of dispersion forces is of special interest in all colloidal systems, since they can crucially influence the properties and processes of these systems. One potential approach is to describe the London–van der Waals forces in terms of the Hamaker constant, which then poses the challenge of calculating the van der Waals interaction energies between colloidal particles. Noskova et al. have described how Hamaker constants of different NPs in toluene can be determined by AF4 in combination with a Newton algorithm-based iteration process [125].

Membranes and recovery

The interactions between the sample components and the membrane are van der Waals interactions in most cases, but they can also be of an unspecific nature. Retention time shifts, up to several min, have been observed during the separation of TiO_2 NPs on membranes of different materials. The shift was uncorrelated to the membrane ζ-potential, but dependent on the particle size (the larger the diameter, the bigger the particle loss) [126], as observed in other contexts [46, 50, 127]. In these cases, the lower recovery observed for the bigger particles was ascribed to the greater probability that they would irreversibly interact with the membrane. This is because they are located closer to the accumulation wall with respect to the smaller particles [46, 50, 126, 127]. When the interactions are strong enough to cause an irreversible adsorption, the sample recoveries decrease and the lifetime of the membrane shortens because of membrane fouling. Mass losses in AF4 were examined for Ag NPs [30, 50], Au NPs [128, 129], TiO_2 NPs [130], SiO_2 NPs [46], and polystyrene PS NPs [127]. The range of the reported recoveries was 53–75% for SiO_2 NPs [46]; 69.5–97.7% or 88–100% for Ag NPs [29, 50], both by using 10 kDa regenerated cellulose membranes; and 50 − 95% for AuNPs

on polyethersulfone 10 kDa MWCO membrane [128].

To compensate for possible losses due to interactions between the NPs and the membrane and/or other wetted surfaces in the flow path of the instrument, the recovery can be evaluated by injecting NP standards through the channel (pre-channel injection) and comparing the peak areas of fractionated and non-fractionated samples (with and without cross-flow, respectively). This procedure is preferred to post-channel injection because it produces calibration curves under exactly the same conditions as a sample run. Alternatively, to minimize membrane fouling and improve NP recovery, both the membrane and the NPs can be functionalized. Recoveries of 99.1(±0.5)%, and a detection limit of 6 μg/kg were achieved by stabilizing AuNPs with phosphine molecules self-assembled on their surface, and by coating three different types of membrane with a negatively charged polystyrenesulfonate polymer [128].

For the sake of completeness, it must be noted that other experimental parameters can also cause low recovery rates. These include permeation through the membrane, pH, the carrier's chemical composition (e.g., the use of buffers and/or surfactants [127]), and the membrane type (regenerated cellulose, polyethersulfone, PTFE). Unfortunately, all these parameters must be carefully investigated on a case by case basis, depending on the sample characteristics and stability.

Special detectors

One clear advantage of FFF is that it can be coupled to many detectors. As such, the best detector sequence can be chosen as a function of the sample characteristics or the purpose of the analysis (Table 2). Two interesting proposals in this regard are NTA and high-resolution mass spectrometry using an atmospheric photo-ionization interface (HR LTQ Orbitrap MS).

NTA is a *counting* technique, which allows the determination of *number*-based PSDs when used online as a detector. NTA has been tested online to detect SiO_2 NPs in biological serum, where AF4's selectivity was necessary because of the complex matrix [131].

The HR LTQ Orbitrap MS has been used online to identify fullerenes in aqueous samples [132]. AF4-MALS can size-characterize fullerenes with both polyhydroxyl and carboxyl surface functional groups [133], but the HR LTQ Orbitrap MS has lower detection and quantification limits (in the range of hundreds ng/L), making this combined technique useful for environmental or ecotoxicology studies [132].

Hollow fiber ~~g~~flow FFF-HF5

HF5 is the miniaturized variant of the F4 technique. In HF5, the separation channel has a cylindrical geometry and consists of an HF membrane with porous walls made of polymeric or ceramic materials. The separation is performed through an external cross-flow applied perpendicularly to a mobile phase flow with an ideally laminar (parabolic) flow profile [134].

In the field of risk assessment for metallic NPs, it is very important to be able to simultaneously distinguish the ionic form from the particulate state. HF5-MALS allows researchers to discriminate between the silver ions and the AgNPs, and to gain information on particle shape by correlating the R_h values determined by HF5 to the R_g values determined by MALS [30]. In the case of low recoveries, the HF5 membranes can also be functionalized (polysulfone membranes functionalized by adding tannic acid to the carrier) [135]. However, the coating procedures must be studied on a case-by-case basis, depending on the NPs and the membrane materials. With respect to AF4, HF5 offers a ready-to-use system with a lower carrier consumption, thanks to the lower cross-flow,

assuring similar recoveries. Nevertheless, AF4 is generally a more versatile system than HF5 [122].

Electrical field flow fractionation and electrical asymmetrical flow-FFF (EAF4)

Another emerging FFF technique is cyclical electrical field flow fractionation (CyElFFF), which is rather promising for the analysis of small colloids. CyElFFF uses cyclical electric fields to characterize and separate NPs based on their size and charge. The high diffusion rate of NPs has prevented CyElFFF from being applicable to particles <100 nm. However, this was recently addressed by using biased cyclical electric fields (BCyElFFF) [~~134~~ 143]. This new method can produce baseline separation of 15 and 40 nm AuNPs. BCyElFFF is a more powerful alternative to standard ElFFF, electrophoresis, and other NP separation and characterization techniques. Moreover, recent improvements in electrical circuitry could lead to its easy miniaturization [136].

Electrical asymmetrical flow-FFF (EAF4) [137] is the FFF family's newest method. It derives from modifying the AF4 channel with an electrical component. EAF4 improves upon AF4 separation and allows electrophoretic mobility (μ) to be measured as a function of size. EAF4 can determine μ for individual populations, which are resolved into separate peaks. This has been demonstrated by the separation of a mixture of three PS latex particles with different sizes, and for the monomer and dimer of BSA and an antibody. EAF4 is suitable for measuring proteins under physiological conditions because it can work with carriers of great ionic strength.

Micro-ThFFF

Micro-thermal field flow fractionation (micro-ThFFF) is a niche technique to separate synthetic, natural, and biological macromolecules, polymers, and particles. The theory is well-described in [138], but its use is limited. It belongs to the miniaturized FFF techniques since the dimensions of the channel are only 0.1 × 3.2 × 76 mm. This microfluidic device was recently used to determine the PSD of an approximately 45 nm photoluminescent diamond, widening the spectrum of potential analytes to include NPs [139].

Concluding remarks

FFF techniques are very versatile tools for sorting and sizing particles in the nano-range. Owing to the wide range of detectors that can be used, FFF techniques can detect and characterize functionalized NPs and colloids in several different matrices, even at very low concentration levels. The absence of a stationary phase means that delicate species can also be analyzed and that sample pretreatment can be reduced. This is particularly critical when evaluating the sample's natural native aggregation state (e.g., for environmental or biochemical determinations).

As highlighted by the practical cases presented in this review, AF4 is by far the most widely used FFF technique for NMs. Sizes and PSDs are usually in good agreement with those obtained using different techniques (TEM, SEM, XRD, MALS, DLS…), although comparison of techniques is not straightforward because different parameters are measured. By showing differences in PSDs, AF4 is also very useful for monitoring particle modifications, such as the adsorption of macromolecules on the surface, or dissolution or aggregation processes. However, despite its broad applicability, several aspects must be improved and further investigated to make AF4 more robust. The membrane technology should be implemented to reduce particle–membrane interactions, which cause shifts in the retention time or, in the worst case of an irreversible adsorption, even sample loss. The particle–membrane interactions also limit the choice of the calibrants necessary to produce accurate qualitative and quantitative PSDs. The analysis times and the solvent consumption could be reduced

if miniaturized separation cartridges were available. At present, researchers have thoroughly evaluated the performance of a miniaturized AF4 system using Au and Ag NP standards as well as TiO_2 particle mixtures with a wide size distribution [140]. However, it is undeniable that miniaturization could have a positive impact on FFF's diagnostic or online processing capabilities.

The role of the other FFF techniques in NP characterization is still limited. This is partially attributable to their scarce availability in research labs and/or because the commercially available fields do not fit the current research trends. This is the case with G-Splitt FFF (gravitational split-flow lateral transport thin fractionation) [141], which would benefit from the application of a strong centrifugal field [142].

Acknowledgements

This work was funded by the University of Ferrara (Fondo di Ateneo per la Ricerca Scientifica) FAR 2016.

Compliance with ethical standards

Conflict of interest disclosure The author certifies that she has no affiliations with or involvement in any organization or entity with any financial interest or nonfinancial interest in the subject matter or materials discussed in this manuscript.

References

1.
AQ2
Giddings JC. A new separation concept based on a coupling of concentration and flow nonuniformities. Sep Sci. 1966;1:123–5.

2. Feynman RP. There's plenty of room at the bottom. Eng Sci. 1960;23(5):22–36.

3. Boverhof DR, Bramante CM, Butala JH, Clancy SF, Lafranconi M, West J, et al. Comparative assessment of nanomaterial definitions and safety evaluation consideration. Regul Toxicol Pharmacol. 2015;73(1):137–50.

4. Weissig V, Pettinger TK, Murdock N. Nanopharmaceuticals (Part 1): products on the market. Int J Nanomedicine. 2014;9:4357–73.

5. Rauscher H, Roebben G, Amenta V, Boix Sanfeliu A, Calzolai L, Emons H, et al. Towards a review of the EC Recommendation for a definition of the term "nanomaterial" Part 1: compilation of information concerning the experience with the definition, JRC Scientific and Policy Report. In: Rauscher, H, Roebben G, editors. EUR 26567 EN. 2014.

6. Roebben G, Rauscher H, Amenta V, Aschberger K, Boix Sanfeliu A, Calzolai L, et al. Towards a review of the EC Recommendation for a definition of the term "nanomaterial" Part 2: assessment of collected information concerning the experience with the definition, JRC Scientific and Policy Report. In: Roebben G, Rauscher H, editors. EUR 26744 EN. 2014.

7. EU commission recommendation – 18 Oct. Recommendations on the definition of nanomaterial Official Journal of the European Union (2011/696/EU). 2011.

8. I.T. 80004-1:2010(E). In: I.O.f. Standardization, editor. Nanotechnologies—vocabulary—part 1: core terms, ISO/TS 80004-1:2010(E). Geneva, Switzerland; 2010.

9. I.T. 27687.2008(E). In: I.O.f. Standardization, editor. Nanotechnologies—terminology and definitions for nano-objects—nanoparticle, nanofiber, and nanoplate, ISO/TS 27687:2008(E). Geneva, Switzerland; 2008.

10. Dudkiewicz A, Wagner S, Lehner A, Chaudhry Q, Pietravalle S, Tiede K, et al. A uniform measurement expression for cross method comparison of nanoparticle aggregate size distributions. Analyst. 2015;140:257–5267.

11. Linsinger TPJ, Roebben G, Gilliland D, Calzolai L, Rossi F, Gibson N, et al. Requirements on measurements for the implementation of the European Commission definition of the term “nanometarial”. Joint Research Centre, Institute for Reference Materials and Measurements (IRMM). 2012. Available at http://publications.jrc.ec.europa.eu/repository /bitstream/JRC73260/irmm_nanomaterials%20(online).pdf. (Accessed 13 Jan 2017)
AQ3

12. Scientific Committee on Consumer Safety (SCCS). Guidance on the safety assessment of nanomaterials in cosmetics. SCCS/1484/12. 2012.

13. Scientific Committee EFSA. Scientific Opinion on Guidance on the risk assessment of the application of nanoscience and nanotechnologies in the food and feed chain. EFSA J. 2011;9(5):2140. doi: 10.2903/j.efsa.2011.2140 . **36 pp**.

14. Schimpf ME, Caldwell K, Giddings JC. Field flow fractionation handbook. New York: Wiley; 2000.

15. Williams S, Kim R, Caldwell KD. Field flow fractionation in biopolymer analysis. Wien: Springer; 2012.

16. Hovingh ME, Thompson GE, Giddings JC. Column parameters in thermal field flow fractionation. Anal Chem. 1970;42:195–203.

17. Giddings JC, Yang FJF, Myers MN. Sedimentation field flow fractionation. Anal Chem. 1974;46:1917–24.

18. Giddings JC, Yang FJF, Myers MN. Flow field flow fractionation: a versatile new separation method. Science. 1976;193:1244–5.

19. Huang Y, Wang X-B, Becker FF, Gascoyne PRC. Introducing di-electrophoresis as a new force field for field flow fractionation. Biophys J. 1997;73(2):1118–29.

20. Castro A, Hoyos M. Study of the onset of the acoustic streaming in parallel plate resonators with pulse ultrasound. Ultrasonics. 2016;66:166–71.

21. Contado C. Nanomaterials in consumer products: a challenging analytical problem. Front Chem. 2015;3:48–67.

22. Laborda F, Bolea E, Cepriá G, Gómez MT, Jiménez MS, Pérez-Arantegui J, et al. Detection,

characterization, and quantification of inorganic engineered nanomaterials: a review of techniques and methodological approaches for the analysis of complex samples. Anal Chim Acta. 2016;904:10–32.

23. Pitkänen L, Striegel AM. Size-exclusion chromatography of metal nanoparticles and quantum dots. TrAC Trends Anal Chem. 2016;80:311–20.

24. Rakcheev D, Philippe A, Schaumann GE. Hydrodynamic chromatography coupled with single particle-inductively coupled plasma mass spectrometry for investigating nanoparticles agglomerates. Anal Chem. 2013;85:10643–7.

25. Philippe A, Schaumann GE. Evaluation of hydrodynamic chromatography coupled with UV-visible fluorescence and inductively coupled plasma mass spectrometry detectors for sizing and quantifying colloids in environmental media. PLoS ONE. 2014;9(2), e90559. doi: 10.1371/journal.pone.0090559 .

26. Striegel MA. Hydrodynamic chromatography: packed columns, multiple detectors, and microcapillaries. Anal Bioanal Chem. 2012;402(1):77–81.

27. Aguirre M, Paulis M, Leiza JR. Particle nucleation and growth in seeded semi batch mini emulsion polymerization of hybrid CeO_2/acrylic latexes. Polymer. 2014;55:752–61.

28. Gray EP, Bruton TA, Higgins CP, Halden RU, Westerhoff P, Ranville JF. Analysis of gold nanoparticle mixtures: a comparison of hydrodynamic chromatography (HDC) and asymmetrical flow field flow fractionation (AF4) coupled to ICP-MS. J Anal At Spectrom. 2012;27:1532–9.

29. Cascio C, Gilliland D, Rossi F, Calzolai L, Contado C. Critical experimental evaluation of key methods to detect, size, and quantify nanoparticulate silver. Anal Chem. 2014;86:12143–51.

30. Marassi V, Casolari S, Roda B, Zattoni A, Reschiglian P, Panzavolta S, et al. Hollow-fiber flow field flow fractionation and multi-angle light scattering investigation of the size, shape, and metal-release of silver nanoparticles in aqueous medium for nano-risk assessment. J Pharm Biomed Anal. 2015;106:92–9.

31. Calzolai L, Gilliland D, Garcìa CP, Rossi F. Separation and characterization of gold nanoparticle mixtures by flow field flow fractionation. J Chromatogr A. 2011;1218(27):4234–9.

32. Laborda F, Bolea E, Jiménez-Lamana J. Single particle inductively coupled plasma mass spectrometry: a powerful tool for nanoanalysis. Anal Chem. 2014;86(5):2270–8.

33. Montaño MD, Badiei HR, Bazargan S, Ranville JF. Improvements in the detection and characterization of engineered nanoparticles using spICP-MS with microsecond dwell times. Environ Sci Nano. 2014;1:338–46.

34. Montaño MD, Olesik JW, Barber AG, Challis K, Ranville JF. Single particle ICP-MS: advances toward routine analysis of nanomaterials. Anal Bioanal Chem. 2016;408:5053–74.

35. Von der Kammer F, Baborowski M, Friese K. Field flow fractionation coupled to multi-angle laser light scattering detectors: applicability and analytical benefits for the analysis of environmental colloids. Anal Chim Acta. 2005;552:166–74.

36. Tadjiki S. Field flow fractionation with single particle ICP-MS as online detector. 2016. Available at: http://www.agilent.com/cs/library/applications/5991-6515EN_v2.pdf . Accessed 28 Nov 2016.

37. Liu W, Jack R, Kutscher D, McSheehy-Ducos S (2015) Evaluation of field flow fractionation-ICP-MS and single particle-ICP-MS for nanoparticle characterization. Available at: http://nemc.us/docs/2015/presentations/Thu-Topics%20in%20Drinking%20Water-24.5-Jack.pdf . Accessed 28 Nov 2016

38. Bohren CF, Huffman DR. Absorption and scattering of light by small particles. New York: Wiley; 1983.

39. Chen B, Beckett R. Development of SdFFF–ETAAS for characterizing soil and sediment colloids. Analyst. 2001;126:1588–93.

40. Runyona JR, Ulmius M, Nilsson L. A perspective on the characterization of colloids and macromolecules using asymmetrical flow field flow fractionation. Colloids Surf A Physicochem Eng Asp. 2014;442:25–33.

41. Pornwilard M-Ma, Siripinyanond A. Field flow fractionation with inductively coupled plasma mass spectrometry: past, present, and future. J Anal At Spectrom. 2014;29:1739–52.

42. Messaud FA, Sanderson RD, Runyon JR, Otte T, Pasch H, Ratanathanawongs Williams SK. An overview on field flow fractionation techniques and their applications in the separation and characterization of polymer. Prog Polym Sci. 2009;34(4):351–68.

43. Roda B, Zattoni A, Reschiglian P, Moon MH, Mirasoli M, Michelini E, et al. Field flow fractionation in bioanalysis: a review of recent trends. Anal Chim Acta. 2009;635(2):132–43.

44. Estelrich J, Quesada-Pérez M, Forcada J, Callejas-Fernández J. Introductory aspects of soft nanoparticles. In soft nanoparticles for biomedical applications. 2014;1–18.

45. Efsa, ANS Panel (EFSA Panel on Food Additives and Nutrient Sources Added to Food). Scientific opinion on the reevaluation of silver (E 174) as food additive. EFSA J. 2016;14(1):4364. doi: 10.2903/j.efsa.2016.4364 .

46. Barahona F, O-Jimenez I, Geiss O, Gilliland D, Barrero-Moreno J. Multimethod approach for the detection and characterisation of food-grade synthetic amorphous silica nanoparticles. J Chromatogr A. 2016;1432:92–100.

47. Regulation (EU) No 1169/2011. On the provision of food information to consumers. Off J Eur Union, L 3014/18. 2011.

48. Contado C, Mejia J, Lozano García O, Piret J-P, Dumortier E, Toussaint O, et al. Physicochemical and toxicological evaluation of silica nanoparticles suitable for food and consumer products collected by following the EC recommendation. Anal Bioanal Chem. 2016;408:271–86.

49. Barahona F, Geiss O, Urbán P, O-Jimenez I, Gilliland D, Barrero-Moreno J. Simultaneous determination of size and quantification of silica nanoparticles by asymmetric flow field flow

fractionation coupled to ICPMS using silica nanoparticles standards. Anal Chem. 2015;87:3039–47.

50. Geiss O, Cascio C, Gilliland D, Franchini F, Barrero-Moreno J. Size and mass determination of silver nanoparticles in an aqueous matrix using asymmetric flow field flow fractionation coupled to inductively coupled plasma mass spectrometer and ultraviolet-visible detectors. J Chromatogr A. 2013;1321:100–8.

51. López-Heras I, Madrid Y, Cámara C. Prospects and difficulties inTiO_2 nanoparticles analysis in cosmetic and food products using asymmetrical flow field flow fractionation hyphenated to inductively coupled plasma mass spectrometry. Talanta. 2014;124:71–8.

52. Ramos K, Ramos L, Cámara C, Gómez-Gómez MM. Characterization and quantification of silver nanoparticles in nutraceuticals and beverages by asymmetric flow field flow fractionation coupled with inductively coupled plasma mass spectrometry. J Chromatogr A. 2014;1371:227–36.

53. Contado C, Ravani L, Passarella M. Size characterization by sedimentation field flow fractionation of silica particles used as food additives. Anal Chim Acta. 2013;788:183–92.

54. Heroult J, Nischwitz V, Bartczak D, Goenaga-Infante H. The potential of asymmetric flow field flow fractionation hyphenated to multiple detectors for the quantification and size estimation of silica nanoparticles in a food matrix. Anal Bioanal Chem. 2014;406:3919–27.

55. Peters RJB, van Bemmel G, Herrera-Rivera Z, Helsper HPFG, Marvin HJP, Weigel S, et al. Characterization of titanium dioxide nanoparticles in food products: analytical methods to define nanoparticles. J Agric Food Chem. 2014;62:6285–93.

56. Grombe R, Charoud-Got J, Emteborg H, Linsinger TPJ, Seghers J, Wagner S, et al. Production of reference materials for the detection and size determination of silica nanoparticles in tomato soup. Anal Bioanal Chem. 2014;406:3895–907.

57. Loeschner K, Navratilova J, Grombe R, Linsinger TPJ, Købler C, Mølhave K, et al. In-house validation of a method for determination of silver nanoparticles in chicken meat based on asymmetric flow field flow fractionation and inductively coupled plasma mass spectrometric detection. Food Chem. 2015;181:78–84.

58. Loeschner K, Navratilova J, Købler C, Mølhave K, Wagner S, von der Kammer F, et al. Detection and characterization of silver nanoparticles in chicken meat by asymmetric flow field flow fractionation with detection by conventional or single particle ICP-MS. Anal Bioanal Chem. 2013;405:8185–95.

59. Linsinger TP, Chaudhry Q, Dehalu V, Delahaut P, Dudkiewicz A, Grombe R, et al. Validation of methods for the detection and quantification of engineered nanoparticles in food. Food Chem. 2013;138(2/3):1959–66.

60. Addo Ntim S, Thomas TA, Noonan GO. Influence of aqueous food simulants on potential nanoparticle detection in migration studies involving nano-enabled food-contact substances. Food Addit Contam Part A. 2016;33(5):905–12.

61. Bott J, Störmer A, Franz R. Migration of nanoparticles from plastic packaging materials containing carbon black into foodstuffs. Food Addit Contam Part A. 2014;31(10):1769–82.

62. Wagner M, Holzschuh S, Traeger A, Fahr A, Schubert US. Asymmetric flow field flow fractionation in the field of nanomedicine. Anal Chem. 2014;86:5201–10.

63. Zattoni A, Roda B, Borghi F, Marassi V, Reschiglian P. Flow field- fractionation for the analysis of nanoparticles used in drug delivery. J Pharm Biomed Anal. 2014;87:53–61.

64. Contado C, Vighi E, Dalpiaz A, Leo E. Influence of secondary preparative parameters and aging effects on PLGA particle size distribution: a sedimentation field flow fractionation investigation. Anal Bioanal Chem. 2013;405(2-3):703–11.

65. Puglia C, Bonina F, Rizza L, Cortesi R, Merlotti E, Drechsler M, et al. Evaluation of percutaneous absorption of naproxen from different liposomal formulations. J Pharm Sci. 2010;99(6):2819–29.

66. Esposito E, Ravani L, Mariani P, Contado C, Drechsler M, Puglia C, et al. Curcumin containing monoolein aqueous dispersions: a preformulative study. Mater Sci Eng C Mater Biol Appl. 2013;33(8):4923–34.

67. Jamieson T, Bakhshi R, Petrova D, Pocock R, Imani M, Seifalian AM. Biological applications of quantum dots. Biomaterials. 2007;28(31):4717–32.

68. Bera D, Qian L, Tseng T-K, Holloway PH. Quantum dots and their multimodal applications: a review. Materials. 2010;3(4):2260–345.

69. Kosmella S, Venus J, Hahn J, Prietzel C, Koetz J. Low-temperature synthesis of polyethyleneimine-entrapped CdS quantum dots. Chem Phys Lett. 2014;592:114–9.

70. Tsai D-H, Cho TJ, Del Rio FW, Gorham JM, Zheng J, Tan J, et al. Controlled formation and characterization of dithiothreitol-conjugated gold nanoparticle clusters. Langmuir. 2014;30:3397–405.

71. Lemke K, Prietzel C, Koetz J. Fluorescent gold clusters synthesized in a poly(ethyleneimine) modified reverse micro-emulsion. J Colloid Interface Sci. 2013;394:141–6.

72. Tsai D-H, Lu Y-F, Del Rio FW, Cho TJ, Guha S, Zachariah MR, et al. Orthogonal analysis of functional gold nanoparticles for biomedical applications. Anal Bioanal Chem. 2015;407:8411–22.

73. Moquin A, Neibert KD, Maysinger D, Winnik FM. Quantum dot agglomerates in biological media and their characterization by asymmetrical flow field flow fractionation. Eur J Pharm Biopharm. 2015;89:290–9.

74. Moquin A, Hutter E, Choi AO, Khatchadourian A, Castonguay A, Winnik FM, et al. Caspase-1 activity in microglia stimulated by pro-inflammagen nanocrystals. ACS Nano. 2013;7(11):9585–98.

75. Menendez-Miranda M, Fernandez-Arguelles MT, Costa-Fernandez JM, Encinar JR,

Sanz-Medel A. Elemental ratios for characterization of quantum-dots populations in complex mixtures by asymmetrical flow field flow fractionation online coupled to fluorescence and inductively coupled plasma mass spectrometry. Anal Chim Acta. 2014;839:8–813.

76. Krystek P, Kettler K, van der Wagt B, de Jong WH. Exploring influences on the cellular uptake of medium-sized silver nanoparticles into THP-1 cells. Microchem J. 2015;120:45–50.

77. Menéndez-Miranda M, Encinar JR, Costa-Fernández JM, Sanz-Medel A. Asymmetric flow field flow fractionation coupled to inductively coupled plasma mass spectrometry for the quantification of quantum dots bioconjugation efficiency. J Chromatogr A. 2015;1422:247–52.

78. Horie M, Kato H, Iwahashi H. Cellular effects of manufactured nanoparticles: effect of adsorption ability of nanoparticles. Arch Toxicol. 2013;87:771–81.

79. Kim ST, Lee Y-J, Hwang Y-S, Lee S. Study on aggregation behavior of cytochrome *c*-conjugated silver nanoparticles using asymmetrical flow field flow fractionation. Talanta. 2015;132:939–44.

80. Hansen M, Smith MC, Crist RM, Clogston JD, McNeil SE. Analyzing the influence of PEG molecular weight on the separation of PEGylated gold nanoparticles by asymmetric-flow field flow fractionation. Anal Bioanal Chem. 2015;407:8661–72.

81. Majewski AP, Stahlschmidt U, Jérôme V, Freitag R, Müller AHE, Schmalz H. PDMAEMA-grafted core−shell−corona particles for nonviral gene delivery and magnetic cell separation. Biomacromolecules. 2013;14:3081–90.

82. Haladjova E, Rangelov S, Geisler M, Boye S, Lederer A, Mountrichas G, et al. Asymmetric flow field flow fractionation investigation of magnetopolyplexes. Macromol Chem Phys. 2015;216:1862–7.

83. Löwa N, Knappe P, Wiekhorst F, Eberbeck D, Thünemann AF, Trahms L. Hydrodynamic and magnetic fractionation of superparamagnetic nanoparticles for magnetic particle imaging. J Magn Magn Mater. 2014;380:266–70.

84. Ashby J, Schachermeyer S, Pan S, Zhong W. Dissociation-based screening of nanoparticle–protein interaction via flow field flow fractionation. Anal Chem. 2013;85:7494–501.

85. Belete A, Maeder K. Novel aqueous nano-scaled formulations of oleic acid stabilized hydrophobic superparamagnetic iron oxide nanocrystals. Drug Dev Ind Pharm. 2013;39(2):186–96.

86. Soshnikova YM, Roman SJ, Chebotareva NA, Baum OI, Obrezkova MV, Gillis RB, et al. Starch-modified magnetite nanoparticles for impregnation into cartilage. J Nanopart Res. 2013;15:2092–101.

87. Issa B, Obaidat IM, Albiss BA, Haik Y. Magnetic nanoparticles: surface effects and properties related to biomedicine applications. Int J Mol Sci. 2013;14:21266–305.

88. Dou H, Kim B-J, Choi S-H, Jung EC, Lee S. Effect of size of Fe_3O_4 magnetic nanoparticles on electrochemical performance of screen printed electrode using sedimentation field flow

fractionation. J Nanopart Res. 2014;16:2679–90.

89. Zataray J, Aguirre A, de la Cal JC, Leiz JR. Polymerization of *N*-vinyl formamide in homogeneous and heterogeneous media and surfactant free emulsion polymerization of MMA using polyvinylamine as stabilizer. Macromol Symp. 2013;333:80–92.

90. Ou C-W, Su C-H, Jeng U-S, S-h H. Characterization of biodegradable polyurethane nanoparticles and thermally induced self-assembly in water dispersion. ACS Appl Mater Interfaces. 2014;6:5685–94.

91. John C, Lange K. Asymmetrical flow field flow fractionation for human serum albumin based nanoparticle characterization and a deeper insight into particle formation processes. J Chromatogr A. 2014;1346:97–106.

92. Engel A, Plöger M, Mulac D, Langer K. Asymmetric flow field flow fractionation (AF4) for the quantification of nanoparticle release from tablets during dissolution testing. Int J Pharm. 2014;461:137–44.

93. Mathaes R, Winter G, Engert J, Besheer A. Application of different analytical methods for the characterization of nonspherical micro- and nanoparticles. Int J Pharm. 2013;453:620–9.

94. Runyon JR, Goering A, Yong K-T, Ratanathanawongs Williams SK. Preparation of narrow dispersity gold nanorods by asymmetrical flow field flow fractionation and investigation of surface plasmon resonance. Anal Chem. 2013;85:940–8.

95. Loeschner K, Harrington CF, Kearney J-L, Langton DJ, Larsen EH. Feasibility of asymmetric flow field flow fractionation coupled to ICP-MS for the characterization of wear metal particles and metalloproteins in biofluids from hip replacement patients. Anal Bioanal Chem. 2015;407:4541–54.

96. Baalousha M, Stolpe B, Lead JR. Flow field–flow fractionation for the analysis and characterization of natural colloids and manufactured nanoparticles in environmental systems: a critical review. J Chromatogr A. 2011;1218(27):4078–103.

97. Regelink IC, Weng L, Koopmans GF, van Riemsdijk WH. Asymmetric flow field–flow fractionation as a new approach to analyze iron-(hydr)oxide nanoparticles in soil extracts. Geoderma. 2013;202–203:134–41.

98. Regelink IC, Voegelin A, Weng L, Koopmans GF, Comans RNJ. Characterization of colloidal Fe from soils using field flow fractionation and Fe K-edge X-ray absorption spectroscopy. Environ Sci Technol. 2014;48:4307–16.

99. Neubauer E, Schenkeveld WDC, Plathe KL, Rentenberger C, von der Kammer F, Kraemer SM, et al. The influence of pH on iron speciation in podzol extracts: iron complexes with natural organic matter and iron mineral nanoparticles. Sci Total Environ. 2013;461(462):108–16.

100. Lapworth DJ, Stolpe B, Williams PJ, Gooddy DC, Lead JR. Characterization of suboxic groundwater colloids using a multimethod approach. Environ Sci Technol. 2013;47:2554–61.

101. Plathe KL, von der Kammer F, Hassellov M, Moore JN, Murayama M, Hofmann T, et al.

The role of nanominerals and mineral nanoparticles in the transport of toxic trace metals: field-flow fractionation and analytical TEM analyses after nanoparticle isolation and density separation. Geochim Cosmochim Acta. 2013;102:213–25.

102. Serrano S, Gomez-Gonzalez MA, O'Day PA, Laborda F, Bolea E, Garrido F. Arsenic speciation in the dispersible colloidal fraction of soils from a mine-impacted creek. J Hazard Mater. 2015;286:30–40.

103. Neubauer E, von der Kammer F, Knorr K-H, Peiffer S, Reichert M, Hofmann T. Colloid-associated export of arsenic in stream water during stormflow events. Chem Geol. 2013;352:81–91.

104. Neubauer E, von der Kammer F, Hofmann T. Using FLOWFFF and HPSEC to determine trace metal-colloid associations in wetland runoff. Water Res. 2013;47:2757–69.

105. Baken S, Regelink IC, Comans RNJ, Smolders E, Koopmans GF. Iron-rich colloids as carriers of phosphorus in streams: a field-flow fractionation study. Water Res. 2016;99:83–90.

106. Chekli L, Phuntsho S, Roy M, Lombi E, Donner E, Kyong Shon H. Assessing the aggregation behavior of iron oxide nanoparticles under relevant environ mental conditions using a multi-method approach. Water Res. 2013;47:4585–99.

107. Chekli L, Phuntsho S, Roy M, Kyong Shon H. Characterization of Fe-oxide nanoparticles coated with humic acid and Suwannee River natural organic matter. Sci Total Environ. 2013;461–462:19–27.

108. Mudalige TK, Qu H, Linder SW. Asymmetric flow-field flow fractionation hyphenated ICP-MS as an alternative to cloud point extraction for quantification of silver nanoparticles and silver speciation: application for nanoparticles with a protein corona. Anal Chem. 2015;87:7395–401.

109. Meisterjahn B, Neubauer E, Von der Kammer F, Hennecke D, Hofmann T. Asymmetrical flow-field-flow fractionation coupled with inductively coupled plasma mass spectrometry for the analysis of gold nanoparticles in the presence of natural nanoparticles. J Chromatogr A. 2014;1372:204–11.

110. Gigault J, Hackley VA. Differentiation and characterization of isotopically modified silver nanoparticles in aqueous media using asymmetric-flow field flow fractionation coupled to optical detection and mass spectrometry. Anal Chim Acta. 2013;763:57–66.

111. Krystek P, Bäuerlein PS, Kooij PJF. Analytical assessment about the simultaneous quantification of releasable pharmaceutical relevant inorganic nanoparticles in tap water and domestic waste water. J Pharm Biomed Anal. 2015;106:116–23.

112. Antonio DC, Cascio C, Jaksic Z, Jurasin D, Lyons DM, Nogueira AJA, et al. Assessing silver nanoparticles behavior in artificial seawater by mean of AF4 and spICP-MS. Mar Environ Res. 2015;111:162–9.

113. Chekli L, Roy M, Tijing LD, Donner E, Lombi E, Shon HK. Agglomeration behavior of titanium dioxide nanoparticles in river waters: a multi-method approach combining light

scattering and field-flow fractionation techniques. J Environ Manag. 2015;159:135–42.

114. Koopmans GF, Hiemstra T, Regelink IC, Molleman B, Comans RNJ. Asymmetric flow field flow fractionation of manufactured silver nanoparticles spiked into soil solution. J Chromatogr A. 2015;1392:100–9.

115. Poda AR, Kennedy AJ, Cuddy MF, Bednar AJ. Investigations of UV photolysis of PVP-capped silver nanoparticles in the presence and absence of dissolved organic carbon. J Nanopart Res. 2013;15:1673–82.

116. Harmon AR, Kennedy AJ, Poda AR, Bednar AJ, Chappell MA, Steevens JA. Determination of nanosilver dissolution kinetics and toxicity in an environmentally relevant aqueous medium. Environ Toxicol Chem. 2014;33(8):1783–91.

117. Krystek P, Brandsma S, Leonards P, Boer J. Exploring methods for compositional and particle size analysis of noble metal nanoparticles in *Daphnia magna*. Talanta. 2016;147:289–95.

118. Coleman JG, Kennedy AJ, Bednar AJ, Ranville JF, Laird JG, Harmon AR, et al. Comparing the effects of nanosilver size and coating variations on bioavailability, internalization, and elimination, using *Lumbriculus variegates*. Environ Toxicol Chem. 2013;32(9):2069–77.

119. Carew AC, Hoque ME, Metcalfe CD, Peyrot C, Wilkinson KJ, Helbing CC. Chronic sublethal exposure to silver nanoparticles disrupts thyroid hormone signaling during *Xenopus laevis* metamorphosis. Aquat Toxicol. 2015;159:99–108.

120. Dou H, Jung EC, Lee S. Factors affecting measurement of channel thickness in asymmetrical flow field flow fractionation. J Chromatogr A. 2015;1393:115–21.

121. Meisterjahn B, Wagner S, von der Kammer F, Hennecke D, Hofmann T. Silver and gold nanoparticle separation using asymmetrical flow field flow fractionation: influence of run conditions and of particle and membrane charges. J Chromatogr A. 2016;1440:150–9.

122. Sánchez-García L, Bolea E, Laborda F, Cubel C, Ferrer P, Gianolio D, et al. Size determination and quantification of engineered cerium oxide nanoparticles by flow field-flow fractionation coupled to inductively coupled plasma mass spectrometry. J Chromatogr A. 2016;1438(18):205–15.

123. Gigault J, Hackley VA. Observation of size-independent effects in nanoparticle retention behavior during asymmetric-flow field-flow fractionation. Anal Bioanal Chem. 2013;405:6251–8.

124. Gigault J, Nguyen TM, Pettibone JM, Hackley VA. Accurate determination of the size distribution for polydisperse, cationic metallic nanomaterials by asymmetric-flow field flow fractionation. J Nanopart Res. 2014;16:2735–44.

125. Noskova S, Scherera C, Maskos M. Determination of Hamaker constants of polymeric nanoparticles in organic solvents by asymmetrical flow field flow fractionation. J Chromatogr A. 2013;1274:151–8.

126. Bendixen N, Losert S, Adlhart C, Lattuad M, Ulrich A. Membrane–particle interactions in an asymmetric flow field flow fractionation channel studied with titanium dioxide nanoparticles.

J Chromatogr A. 2014;1334:92–100.

127. Schachermeyer S, Ashby J, Kwon M, Zhong W. Impact of carrier fluid composition on recovery of nanoparticles and proteins in flow field flow fractionation. J Chromatogr A. 2012;1264:72–9.

128. Mudalige TK, Qu H, Sánchez-Pomales G, Sisco PN, Linder SW. Simple functionalization strategies for enhancing nanoparticle separation and recovery with asymmetric flow field flow fractionation. Anal Chem. 2015;87:1764–72.

129. Schmidt B, Loeschner K, Hadrup N, Mortensen A, Sloth JJ, Koch CB, et al. Quantitative characterization of gold nanoparticles by field-flow fractionation coupled online with light scattering detection and inductively coupled plasma mass spectrometry. Anal Chem. 2011;83(7):2461–8.

130. Nischwitz V, Goenaga-Infante H. Improved sample preparation and quality control for the characterisation of titanium dioxide nanoparticles in sunscreens using flow field flow fractionation on- line with inductively coupled plasma mass spectrometry. J Anal At Spectrom. 2012;27(1):1084–92.

131. Bartczak D, Vincent P, Goenaga-Infante H. Determination of size- and number-based concentration of silica nanoparticles in a complex biological matrix by online techniques. Anal Chem. 2015;87:5482–5.

132. Herrero P, Bäuerlein PS, Emke E, Pocurull E, de Voogt P. Asymmetrical flow field-flow fractionation hyphenated to Orbitrap high resolution mass spectrometry for the determination of (functionalized) aqueous fullerene aggregates. J Chromatogr A. 2014;1356:277–82.

133. Astefanei A, Kok WT, Bäuerlein P, Núnez O, Galceran MT, de Voogt P, et al. Characterization of aggregates of surface modified fullerenes by asymmetrical flow field-flow fractionation with multi-angle light scattering detection. J Chromatogr A. 2015;1408:197–206.

134. Reschiglian P, Roda B, Zattoni A, Min BR, Moon MH. High performance, disposable hollow fiber flow field flow fractionation for bacteria and cells. First application to deactivated *Vibrio cholerae*. J Sep Sci. 2002;25:490–8.

135. Saenmuangchin R, Mettakoonpitak J, Shiowatana J, Siripinyanond A. Separation of silver nanoparticles by hollow fiber flow field flow fractionation: addition of tannic acid into carrier liquid as a modifier. J Chromatogr A. 2015;1415:115–22.

136. Tasci TO, Johnson WP, Fernandez DP, Manangon E, Gale BK. Circuit modification in electrical field flow fractionation systems generating higher resolution separation of nanoparticles. J Chromatogr A. 2014;1365:164–72.

137. Johann C, Elsenberg S, Schuch H, Rösch U. Instrument and method to determine the electrophoretic mobility of nanoparticles and proteins by combining electrical and flow field flow fractionation. Anal Chem. 2015;87:4292–8.

138. Janča J. Microthermal field-flow fractionation: analysis of synthetic, natural, and biological macromolecules and particles. New York: HNB Publishing; 2008.

139. Janča J. Characterization of diamond nanoparticles by high-speed micro-thermal field-flow fractionation. Int J Polym Anal Charact. 2015;20:671–80.

140. Müller D, Cattaneo S, Meier F, Welz R, de Mello AJ. Nanoparticle separation with a miniaturized asymmetrical flow field-flow fractionation cartridge. Front Chem. 2015. Available at: http://dx.doi.org/10.3389/fchem.2015.00045 . Accessed 8 Dec 2016.

141. Contado C, Hoyos M. SPLITT cell analytical separation of silica particles. Non-specific crossover effects: does the shear-induced diffusion play a role? Chromatographia. 2007;65(7):453–62.

142. Camerani MC, Steenari BM, Sharma R, Beckett R. Cd speciation in biomass fly ash particles after size separation by centrifugal SPLITT. Fuel. 2002;81(13):1739–53.

143. Tasci TO, Johnson WP, Fernandez DP, Manangon E, Gale BK. Biased cyclical electrical field flow fractionation for separation of sub 50 nm particles. Anal Chem. 2013;85:11225–32.
AQ4